Hindawi
Shock and Vibration
Volume 2023, Article ID 7020462, 19 pages
https://doi.org/10.1155/2023/7020462

Research Article

Two-Layer Parallel Fuzzy Logic Controller Design for Semiactive Suspension System with a Full Car Model

Vu Van Tan

Department of Automotive Mechanical Engineering, Faculty of Mechanical Engineering, University of Transport and Communications, Hanoi 100000, Vietnam

Correspondence should be addressed to Vu Van Tan; vvtan@utc.edu.vn

Received 1 July 2022; Revised 13 October 2022; Accepted 16 May 2023; Published 24 May 2023

Academic Editor: Francisco Beltran-Carbajal

This paper presents research results on semiactive suspension using a fuzzy logic controller. Firstly, a full car model is built with 7 degrees of freedom using a semiactive suspension system at all four wheels. The dynamic equations are converted to the state space representation to facilitate control design and improve accuracy in simulation design. Then, a two-layer parallel fuzzy logic controller is designed with 49 and 25 rules for two fuzzy inference systems. In this way, the fuzzy logic controller is able to respond to a wide operating range of the system and the output force is smoother. Finally, the evaluation results are performed in the frequency and time domains with a real random road profile, and they showed that the root mean square value of the signals when using a semiactive suspension system with the proposed fuzzy logic controller decreased by over 25% compared to the passive suspension system. This clearly demonstrates the effectiveness of the proposed controller in improving the ride comfort, the road holding and ensuring the suspension travel of cars.

1. Introduction

1.1. Background. The suspension system is an important component of automobiles. The two main parts of the suspension system include the elastic element and the damping element (shock absorber) as shown in Figure 1. The elastic element can be a spring, a leaf spring or an air spring; meanwhile, the damping element that quenches the car's vibrations can be passive dampers or controlled dampers (magnetorheological: MR and electrorheological: ER) [1].

Based on the characteristics of the elastic and damping elements, the suspension system is divided into three main types: passive suspension, semiactive suspension, and active suspension [2, 3]. For semiactive suspension, the dampers can be controlled in real time to adjust the damping coefficient. This makes it possible to flexibly switch between the two characteristics of the ride comfort and the road holding. Research and experimental results have shown that because the dampers perform the task of consuming vibrational energy, the semiactive suspension system has a great balance between the goal of improving the vibration quality of the car and fuel consumption. Therefore, the semiactive suspension system is widely used for passenger cars [4].

1.2. Related Works. Research on semiactive suspension systems has been carried out by researchers for nearly 30 years in the main areas including perfecting dampers, control algorithms, and car modeling.

(i) Dampers: in the study of semiactive suspension systems, the characteristics of the dampers (MR, ER) are of interest to many researchers [5–7]. For MR dampers, it uses the physical properties of MR fluids. When a magnetic field is applied to the MR fluid, the particles form chains, resulting in a change in the viscosity of the fluid and a change in the damping coefficient of the suspension system. This type of damper allows different control methods to be used to match the desired performance goals by delivering the appropriate current [8]. Similar to MR dampers, ER dampers are filled with ER fluids, which is a mixture of oil and particles that are very

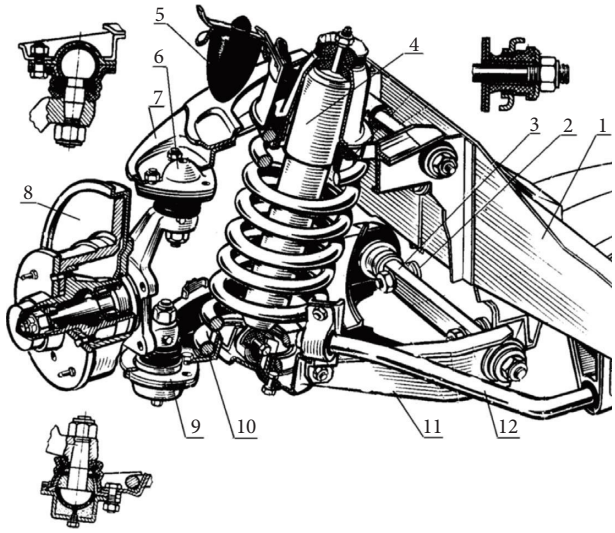

Figure 1: Structural diagram of the car's suspension system [2]. 1-chassis, 2-cushion for tilt adjustment, 3-lower swing arm, 4-damper, 5-limiting lugs, 6-upper ball joint, 7-upper wishbone; 8-brake disc, 9-lower ball joint, 10-spring, 11-lower wishbone, and 12-antiroll bar.

small in size and sensitive to electric fields. Therefore, the volume of the ER liquid changes with the change of the electric field, leading to a change in the damping coefficient [7]. To simplify the research process of the semiactive suspension system, the modeling of these two types of dampers in linear and nonlinear forms has been proposed [9, 10].

(ii) Control algorithms: in order to control the semiactive suspension system, different control methods have been studied and applied. The first research studies that can be mentioned are the Skyhook, Groundhook, and Hybrid control methods proposed by Karnopp et al. [11] and then developed by many researchers at a higher level and with better efficiency [12, 13]. The fuzzy logic control method has been used in semiactive suspension systems, but the construction of the control law is based on the experience of the designer. Therefore, this method has the advantage that it does not depend on the parameters of the system, so it is easy to apply in practice [14, 15]. Modern control methods such as optimal control (LQ, LQR, and LQG), robust control, and model predictive control have been studied and applied to this type of suspension [16–19]. Control methods are applied to the semiactive suspension with the main objective of improving ride comfort and road holding of cars. In addition, special objectives of handling, loading, and suspension travel limit are also considered from different perspectives when studying semiactive suspension control [20, 21]. Recently, the research group of Professor Olivier Sename at Gipsa-lab (Grenoble, France) has developed a research direction of using linear parameter varying (LPV) to control this suspension system and has conducted experiments, as well as evaluated positive results on the INOVE test-bench using ER dampers [22–24].

(iii) Car modeling: the most used studies are the two-degree-of-freedom (DOF) quarter car model with sprung and unsprung masses. This model is not only specific to automobiles but also to oscillating systems in engineering in general. However, this model has the disadvantage that it only considers vibrations in the vertical direction but cannot evaluate in other directions [25, 26]. The pitch and roll half car models were used in the study of semiactive suspension systems to evaluate the vibration quality in two other directions of cars: longitudinal and lateral [27, 28]. For the most general assessment of the effectiveness of the controlled suspension system, the full car model of 7 DOF is considered to be the most accurate and closest to reality [29, 30]. There have been some researchers using this model in suspension control, but most of the studies just stop at the basic level when considering individual criteria. This is also an area of research that needs to be expanded to accurately assess the advantages and disadvantages of the semiactive suspension system.

1.3. Research Contributions. This paper focuses on building a two-layer parallel fuzzy logic controller to control the semiactive suspension system with a full car model, and the main contributions are listed as follows:

(i) A full car model using the semiactive suspension system with 7 degrees of freedom is proposed. In this model, the state vector is selected reasonably to ensure that the output signal includes variables related to the ride comfort, the road holding, and the suspension space. The dynamic equations are converted to the state space form, and matrices are used to perform simulation design. This helps increase accuracy during simulation and evaluation.

(ii) A two-layer parallel fuzzy logic controller is built to ensure that the fuzzy inference output force meets the operating ranges of the system. The first fuzzy inference system consists of 49 rules, while the second fuzzy inference system consists of 25 rules. Both fuzzy inference systems use the input signals related to the sprung mass, the output signal being the damping force. The study also conducted to determine the optimal correlation of the two systems to ensure the most effective control target.

(iii) Simulation results are performed in both time and frequency domains. In the frequency domain, the efficiency of the fuzzy-controlled semiactive suspension is evaluated through the amplitude-frequency transfer function of the signals. In the time domain, the author evaluates through the random road profile measured in practice. The analysis results have shown that the semiactive suspension system using the fuzzy logic controller

has reduced the root mean square value of the signals by more than 25% compared to the car using the passive suspension system.

The structure of the paper is organized as follows: Section 2 introduces a full car model and converts the dynamic equations into the state space form. Section 3 designs a two-layer parallel fuzzy logic controller. The vibration quality and evaluation results in the time and frequency domains are presented in Section 4. Finally, the conclusions are in Section 5.

2. Vehicle Modeling

The most accurate model used to evaluate the vibration quality of an automobile is a full model consisting of an absolutely rigid frame as a sprung mass with 3 degrees of freedom (DOF) and unsprung masses with 4 DOF corresponds to the four vertical displacements of the wheels. In this paper, the author uses a full car model as shown in Figure 2, and the model's parameters are shown in Table 1. In this model, the forces f_{d1}, f_{d2}, f_{d3}, and f_{d4} are those generated by the semiactive dampers.

The dynamic equation of the full car model in the vertical direction is determined in the following equation:

$$\begin{cases} m\ddot{z} = k_{12}(z_1 - z_1') + c_{12}(\dot{z}_1 - \dot{z}_1') - f_{d1} + k_{22}(z_2 - z_2') + c_{22}(\dot{z}_2 - \dot{z}_2') - f_{d2} \\ + k_{32}(z_3 - z_3') + c_{32}(\dot{z}_3 - \dot{z}_3') - f_{d3} + k_{42}(z_4 - z_4') + c_{42}(\dot{z}_4 - \dot{z}_4') - f_{d4}, \\ J_x\ddot{\varphi} = dk_{12}(z_1 - z_1') + dc_{12}(\dot{z}_1 - \dot{z}_1') - df_{d1} + dk_{22}(z_2 - z_2') + dc_{22}(\dot{z}_2 - \dot{z}_2') - df_{d2} \\ - ck_{32}(z_3 - z_3') - cc_{32}(\dot{z}_3 - \dot{z}_3') + cf_{d3} - ck_{42}(z_4 - z_4') - cc_{42}(\dot{z}_4 - \dot{z}_4') + cf_{d4}, \\ J_y\ddot{\theta} = -ak_{12}(z_1 - z_1') - ac_{12}(\dot{z}_1 - \dot{z}_1') + af_{d1} + bk_{22}(z_2 - z_2') + bc_{22}(\dot{z}_2 - \dot{z}_2') - bf_{d2} \\ + bk_{32}(z_3 - z_3') + bc_{32}(\dot{z}_3 - \dot{z}_3') - bf_{d3} - ak_{42}(z_4 - z_4') - ac_{42}(\dot{z}_4 - \dot{z}_4') + af_{d4}, \\ m_1\ddot{z}_1 = -k_{12}(z_1 - z_1') - c_{12}(\dot{z}_1 - \dot{z}_1') + f_{d1} + k_{11}(q_1 - z_1), \\ m_2\ddot{z}_2 = -k_{22}(z_2 - z_2') - c_{22}(\dot{z}_2 - \dot{z}_2') + f_{d2} + k_{21}(q_2 - z_2), \\ m_3\ddot{z}_3 = -k_{32}(z_3 - z_3') - c_{32}(\dot{z}_3 - \dot{z}_3') + f_{d3} + k_{31}(q_3 - z_3), \\ m_4\ddot{z}_4 = -k_{42}(z_4 - z_4') - c_{42}(\dot{z}_4 - \dot{z}_4') + f_{d4} + k_{41}(q_4 - z_4). \end{cases} \tag{1}$$

In equation (1), it should be noted that the displacements of the sprung mass at the position associated with the suspension systems are determined in equation (2). Since the pitch and roll angles of the sprung mass are small under normal conditions of motion, applying the rule for trigonometric functions with small angles, therefore $\tan\varphi \approx \varphi$, $\tan\theta \approx \theta$.

$$\begin{cases} z_1' = z + d\tan\varphi - a\tan\theta \approx z + d\varphi - a\theta, \\ z_2' = z + d\tan\varphi + b\tan\theta \approx z + d\varphi + b\theta, \\ z_3' = z - c\tan\varphi + b\tan\theta \approx z - c\varphi + b\theta, \\ z_4' = z - c\tan\varphi - a\tan\theta \approx z - c\varphi - a\theta, \end{cases} \tag{2}$$

The forces of the semiactive dampers are determined by the relative displacement velocity between the sprung and unsprung masses with the damping coefficient, which is varied according to the control algorithm: $f_{\mathrm{di}} = c_{\mathrm{ei}}(\dot{z}_i' - \dot{z}_i)$ with $i = 1 \div 4$. Generally, there are two main types of dampers, which are used for semiactive suspension systems: magnetorheological (MR) and electrorheological (ER). Based on Guo's model, the dynamical nonlinear model of the ER damper is represented as follows [23]:

$$\tau\dot{f}_d + f_d = \gamma_c u_{\mathrm{nl}}, \tag{3}$$

where $u_{nl} = u\tan(k_1(Z_i' - Z_i) + c_1(\dot{Z}_i' - \dot{Z}_i))$; u is the duty cycle of the PWM signal; $\tau, \gamma_c, k_1, \mathrm{and} c_1$ are the time constant, dynamic yield force of ER fluid, hysteresis coefficient due to displacement, and hysteresis coefficient due to velocity, respectively.

The dynamic equation (1) is written in the state space representation form as follows [32]:

$$\begin{cases} \dot{X} = \mathrm{AX} + \mathrm{BU}, \\ Y = \mathrm{CX} + \mathrm{DU}, \end{cases} \tag{4}$$

where the state vector is as follows:

$$\begin{aligned} X &= \left[z_1 - z_1', z_2 - z_2', z_3 - z_3', z_4 - z_4', z_1, z_2, z_3, z_4, \dot{z}_1, \dot{z}_2, \dot{z}_3, \dot{z}_4, \dot{z}, \dot{\varphi}, \dot{\theta}\right]^T, \\ \Longrightarrow \dot{X} &= \left[\dot{z}_1 - \dot{z}_1', \dot{z}_2 - \dot{z}_2', \dot{z}_3 - \dot{z}_3', \dot{z}_4 - \dot{z}_4', \dot{z}_1, \dot{z}_2, \dot{z}_3, \dot{z}_4, \ddot{z}_1, \ddot{z}_2, \ddot{z}_3, \ddot{z}_4, \ddot{z}, \ddot{\varphi}, \ddot{\theta}\right]^T. \end{aligned} \tag{5}$$

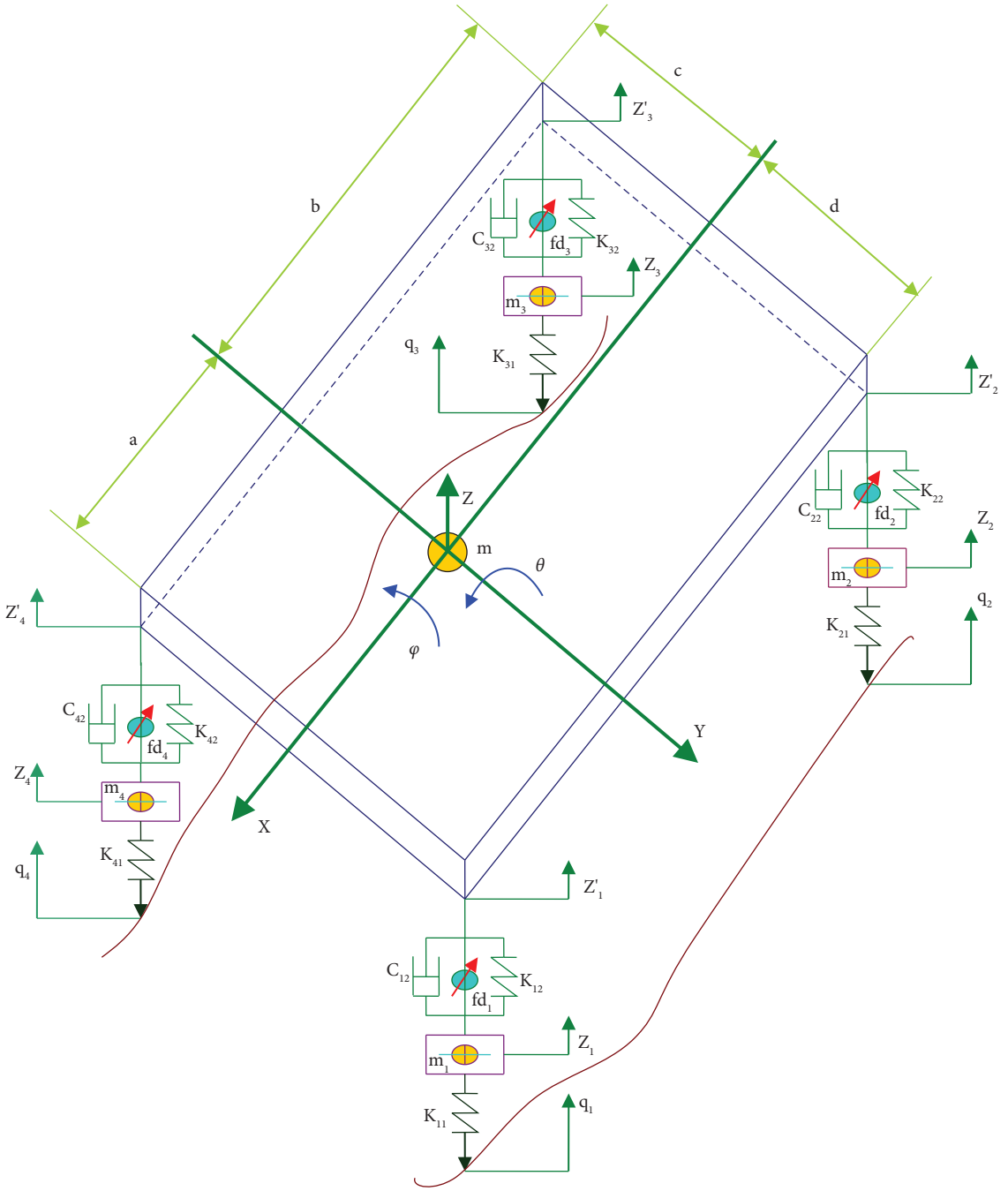

Figure 2: A full car model using the semiactive suspension system.

The variables of the input vector include the disturbances from the road profile and the forces from the semiactive dampers, specifically as follows:

$$U = [q_1, q_2, q_3, q_4, f_{d1}, f_{d2}, f_{d3}, f_{d4}, 0, 0, 0, 0, 0, 0, 0, 0]^T. \quad (6)$$

The three basic criteria used to evaluate the vibration quality of cars include ride comfort, suspension space, and road holding. Therefore, the variables of the output vector include the three accelerations of the sprung mass, the relative displacement between the sprung and unsprung masses, and the interaction forces between the wheel and the road surface $F_{dt\,i} = k_{i1}(q_i - z_i) = k_{i1}q_i - k_{i1}z_i$, specifically as follows [33]:

$$Y = \left[\ddot{z}, \ddot{\varphi}, \ddot{\theta}, -(z_1 - z_1'), -(z_2 - z_2'), -(z_3 - z_3'), -(z_4 - z_4'), -(\dot{z}_1 - \dot{z}_1'), -(\dot{z}_2 - \dot{z}_2'), -(\dot{z}_3 - \dot{z}_3'), -(\dot{z}_4 - \dot{z}_4'), F_{dt1}, F_{dt2}, F_{dt3}, F_{dt4}\right]^T. \quad (7)$$

Table 1: The symbols and parameters of a full car model [31].

Symbols	Description	Value	Unit
m_1, m_4	Unsprung mass at the first, fourth wheels	30.2	kg
m_2, m_3	Unsprung mass at the second, third wheels	49.7	kg
m	Sprung mass	1150	kg
k_{11}, k_{21}, k_{31}, k_{41}	Stiffness coefficient of the tyres	181000	N/m
k_{12}, k_{42}	Stiffness coefficient of front suspension	30000	N/m
k_{22}, k_{32}	Stiffness coefficient of rear suspension	32500	N/m
c_1, c_2, c_3, c_4	Damping coefficient	1400	Ns/m
J_Y	Pitch moment of inertia of sprung mass	861.8	kgm^2
J_X	Roll moment of inertia of sprung mass	330.5	kgm^2
a	Length of the front axle from the CG	1.116	m
b	Length of the rear axle from the CG	1.232	m
d, c	Length of the left/right wheels from the CG	0.621	m

The matrices A and B of the state space representation form in equation (4) are defined as follows: $A = -T^{-1}A_1$; $B = -T^{-1}B_1$

$$T = \begin{bmatrix} -\frac{c_{12}}{m_1} & 0 & 0 & 0 & 0 & 0 & 0 & 0 & -1 & 0 & 0 & 0 & 0 & 0 & 0 \\ 0 & -\frac{c_{22}}{m_2} & 0 & 0 & 0 & 0 & 0 & 0 & 0 & -1 & 0 & 0 & 0 & 0 & 0 \\ 0 & 0 & -\frac{c_{32}}{m_3} & 0 & 0 & 0 & 0 & 0 & 0 & 0 & -1 & 0 & 0 & 0 & 0 \\ 0 & 0 & 0 & -\frac{c_{42}}{m_4} & 0 & 0 & 0 & 0 & 0 & 0 & 0 & -1 & 0 & 0 & 0 \\ \frac{c_{12}}{m} & \frac{c_{22}}{m} & \frac{c_{32}}{m} & \frac{c_{42}}{m} & 0 & 0 & 0 & 0 & 0 & 0 & 0 & 0 & -1 & 0 & 0 \\ \frac{dc_{12}}{J_x} & \frac{dc_{22}}{J_x} & -\frac{cc_{32}}{J_x} & -\frac{cc_{42}}{J_x} & 0 & 0 & 0 & 0 & 0 & 0 & 0 & 0 & 0 & -1 & 0 \\ -\frac{ac_{12}}{J_y} & \frac{bc_{22}}{J_y} & \frac{bc_{32}}{J_y} & -\frac{ac_{42}}{J_y} & 0 & 0 & 0 & 0 & 0 & 0 & 0 & 0 & 0 & 0 & -1 \\ 1 & 0 & 0 & 0 & 0 & 0 & 0 & 0 & 0 & 0 & 0 & 0 & 0 & 0 & 0 \\ 0 & 1 & 0 & 0 & 0 & 0 & 0 & 0 & 0 & 0 & 0 & 0 & 0 & 0 & 0 \\ 0 & 0 & 1 & 0 & 0 & 0 & 0 & 0 & 0 & 0 & 0 & 0 & 0 & 0 & 0 \\ 0 & 0 & 0 & 1 & 0 & 0 & 0 & 0 & 0 & 0 & 0 & 0 & 0 & 0 & 0 \\ 0 & 0 & 0 & 0 & 1 & 0 & 0 & 0 & 0 & 0 & 0 & 0 & 0 & 0 & 0 \\ 0 & 0 & 0 & 0 & 0 & 1 & 0 & 0 & 0 & 0 & 0 & 0 & 0 & 0 & 0 \\ 0 & 0 & 0 & 0 & 0 & 0 & 1 & 0 & 0 & 0 & 0 & 0 & 0 & 0 & 0 \\ 0 & 0 & 0 & 0 & 0 & 0 & 0 & 1 & 0 & 0 & 0 & 0 & 0 & 0 & 0 \end{bmatrix},$$

$$A_1 = \begin{bmatrix} a_{7x8} & 0_{7x7} \\ 0_{8x8} & a_{8x7} \end{bmatrix};$$

$$B_1 = \begin{bmatrix} b_{7x8} & 0_{7x7} \\ 0_{8x8} & 0_{8x7} \end{bmatrix};$$

$$a_{8x7} = \begin{bmatrix} -1 & 0 & 0 & 0 & 1 & d & -a \\ 0 & -1 & 0 & 0 & 1 & d & b \\ 0 & 0 & -1 & 0 & 1 & -c & b \\ 0 & 0 & 0 & -1 & 1 & -c & a \\ -1 & 0 & 0 & 0 & 0 & 0 & 0 \\ 0 & -1 & 0 & 0 & 0 & 0 & 0 \\ 0 & 0 & -1 & 0 & 0 & 0 & 0 \\ 0 & 0 & 0 & -1 & 0 & 0 & 0 \end{bmatrix};$$

$$a_{7x8} = \begin{bmatrix} -\frac{k_{12}}{m_1} & 0 & 0 & 0 & -\frac{k_{12}}{m_1} & 0 & 0 & 0 \\ 0 & -\frac{k_{22}}{m_2} & 0 & 0 & 0 & -\frac{k_{22}}{m_2} & 0 & 0 \\ 0 & 0 & -\frac{k_{32}}{m_3} & 0 & 0 & 0 & -\frac{k_{32}}{m_3} & 0 \\ 0 & 0 & 0 & -\frac{k_{42}}{m_4} & 0 & 0 & 0 & -\frac{k_{42}}{m_4} \\ \frac{k_{12}}{m} & \frac{k_{22}}{m} & \frac{k_{32}}{m} & \frac{k_{42}}{m} & 0 & 0 & 0 & 0 \\ \frac{dk_{12}}{J_x} & \frac{dk_{22}}{J_x} & -\frac{ck_{32}}{J_x} & -\frac{ck_{42}}{J_x} & 0 & 0 & 0 & 0 \\ -\frac{ak_{12}}{J_y} & \frac{bk_{22}}{J_y} & \frac{bk_{32}}{J_y} & -\frac{ak_{42}}{J_y} & 0 & 0 & 0 & 0 \end{bmatrix};$$

$$b_{7x8} = \begin{bmatrix} \frac{k_{11}}{m_1} & 0 & 0 & 0 & \frac{1}{m_1} & 0 & 0 & 0 \\ 0 & \frac{k_{21}}{m_2} & 0 & 0 & 0 & \frac{1}{m_2} & 0 & 0 \\ 0 & 0 & \frac{k_{31}}{m_3} & 0 & 0 & 0 & \frac{1}{m_3} & 0 \\ 0 & 0 & 0 & \frac{k_{41}}{m_4} & 0 & 0 & 0 & \frac{1}{m_4} \\ 0 & 0 & 0 & 0 & -\frac{1}{m} & -\frac{1}{m} & -\frac{1}{m} & -\frac{1}{m} \\ 0 & 0 & 0 & 0 & -\frac{d}{J_x} & -\frac{d}{J_x} & \frac{c}{J_x} & \frac{c}{J_x} \\ 0 & 0 & 0 & 0 & \frac{a}{J_y} & -\frac{b}{J_y} & -\frac{b}{J_y} & \frac{a}{J_y} \end{bmatrix}. \quad (8)$$

The matrices C and D of the state space representation form in equation (4) are defined as follows:

$$C = \left[c_{15x12} \;\; c_{15x3} \right];$$

$$D = \begin{bmatrix} 0_{3x4} & d_{3x4} & 0_{3x7} \\ 0_{8x4} & 0_{8x4} & 0_{8x7} \\ d_{4x4} & 0_{4x4} & 0_{4x7} \end{bmatrix},$$

$$d_{3x4} = \begin{bmatrix} -\frac{1}{m} & -\frac{1}{m} & -\frac{1}{m} & -\frac{1}{m} \\ -\frac{d}{J_x} & -\frac{d}{J_x} & \frac{c}{J_x} & \frac{c}{J_x} \\ \frac{a}{J_y} & -\frac{b}{J_y} & -\frac{b}{J_y} & \frac{a}{J_y} \end{bmatrix};$$

$$d_{4x4} = \begin{bmatrix} k_{11} & 0 & 0 & 0 \\ 0 & k_{21} & 0 & 0 \\ 0 & 0 & k_{31} & 0 \\ 0 & 0 & 0 & k_{41} \end{bmatrix},$$

$$c_{15x12} = \begin{bmatrix} \frac{k_{12}}{m} & \frac{k_{22}}{m} & \frac{k_{32}}{m} & \frac{k_{42}}{m} & 0 & 0 & 0 & 0 & \frac{c_{12}}{m} & \frac{c_{22}}{m} & \frac{c_{32}}{m} & \frac{c_{42}}{m} \\ \frac{dk_{12}}{J_x} & \frac{dk_{22}}{J_x} & -\frac{ck_{32}}{J_x} & -\frac{ck_{42}}{J_x} & 0 & 0 & 0 & 0 & \frac{dc_{12}}{J_x} & \frac{dc_{22}}{J_x} & -\frac{cc_{32}}{J_x} & -\frac{cc_{42}}{J_x} \\ -\frac{ak_{12}}{J_y} & \frac{bk_{22}}{J_y} & \frac{bk_{32}}{J_y} & -\frac{ak_{42}}{J_y} & 0 & 0 & 0 & 0 & -\frac{ac_{12}}{J_y} & \frac{bc_{22}}{J_y} & \frac{bc_{32}}{J_y} & -\frac{ac_{42}}{J_y} \\ -1 & 0 & 0 & 0 & 0 & 0 & 0 & 0 & 0 & 0 & 0 & 0 \\ 0 & -1 & 0 & 0 & 0 & 0 & 0 & 0 & 0 & 0 & 0 & 0 \\ 0 & 0 & -1 & 0 & 0 & 0 & 0 & 0 & 0 & 0 & 0 & 0 \\ 0 & 0 & 0 & -1 & 0 & 0 & 0 & 0 & 0 & 0 & 0 & 0 \\ 0 & 0 & 0 & 0 & 0 & 0 & 0 & 0 & -1 & 0 & 0 & 0 \\ 0 & 0 & 0 & 0 & 0 & 0 & 0 & 0 & 0 & -1 & 0 & 0 \\ 0 & 0 & 0 & 0 & 0 & 0 & 0 & 0 & 0 & 0 & -1 & 0 \\ 0 & 0 & 0 & 0 & 0 & 0 & 0 & 0 & 0 & 0 & 0 & -1 \\ 0 & 0 & 0 & 0 & -k_{11} & 0 & 0 & 0 & 0 & 0 & 0 & 0 \\ 0 & 0 & 0 & 0 & 0 & -k_{21} & 0 & 0 & 0 & 0 & 0 & 0 \\ 0 & 0 & 0 & 0 & 0 & 0 & -k_{31} & 0 & 0 & 0 & 0 & 0 \\ 0 & 0 & 0 & 0 & 0 & 0 & 0 & -k_{41} & 0 & 0 & 0 & 0 \end{bmatrix},$$

$$c_{15x3} = \begin{bmatrix} -\frac{1}{m}(c_{12}+c_{22}+c_{32}+c_{42}) & -\frac{1}{m}(dc_{12}+dc_{22}-cc_{32}-cc_{42}) & -\frac{1}{m}(-ac_{12}+bc_{22}+bc_{32}-ac_{42}) \\ -\frac{1}{J_x}(dc_{12}+dc_{22}-cc_{32}-cc_{42}) & -\frac{1}{J_x}\left(d^2c_{12}+d^2c_{22}+c^2c_{32}+c^2c_{42}\right) & -\frac{1}{J_x}(-adc_{12}+bdc_{22}-bcc_{32}+acc_{42}) \\ -\frac{1}{J_y}(-ac_{12}+bc_{22}+bc_{32}-ac_{42}) & -\frac{1}{J_y}(-adc_{12}+bdc_{22}-bcc_{32}+acc_{42}) & -\frac{1}{J_y}\left(a^2c_{12}+b^2c_{22}+b^2c_{32}+a^2c_{42}\right) \\ 0 & 0 & 0 \\ 0 & 0 & 0 \\ 0 & 0 & 0 \\ 0 & 0 & 0 \\ 1 & d & -a \\ 1 & d & b \\ 1 & -c & b \\ 1 & -c & -a \\ 0 & 0 & 0 \\ 0 & 0 & 0 \\ 0 & 0 & 0 \\ 0 & 0 & 0 \end{bmatrix}. \tag{9}$$

3. Two-Layer Parallel Fuzzy Logic Controller Design

3.1. Defining Input and Output Variables (Linguistic Variables). The main goal in the control of the suspension is to ensure the improvement of the vehicle's the ride comfort and the road holding. Besides, this study proposes a new idea to combine two fuzzy inference systems, which work in tandem so that the damping force determination is softened and covers the entire operating range of the system. The two sensors are used to determine the input signals, which are velocity (Z_s) and acceleration ($\ddot{Z}_s$) of the sprung mass, and the linguistic variables are therefore defined in Table 2.

The actual force of the semiactive damper is determined in the equation as follows:

$$f_d = f_{d1}\left(k_e, k_{\mathrm{ec}}, k_u, E, \mathrm{EC}\right) + \chi\left(f_{d2}\left(k_e, k_{\mathrm{ec}}, k_u, e, \mathrm{ec}\right)\right), \tag{10}$$

where $f_{d1}(k_e, k_{ec}, k_u, E, \mathrm{EC})$ is the damping force according to the first fuzzy inference system E, EC, U; $f_{d2}(k_e, k_{ec}, k_u, e, \mathrm{ec})$ is the damping force according to the second fuzzy inference system e, ec, u; k_e, k_{ec} is the scale factor for fuzzification; k_u is the scale factor for defuzzification; χ-weights represent the role of the fuzzy inference system e, ec, u.

3.2. The Fuzzy Inference System E, EC, U. The physical value domain of the input variables is selected as follows: the velocity of the sprung mass $\dot{Z}_s$, E: $[-7 \div 7]$ (m/s) and the acceleration of the sprung mass $\ddot{Z}_s$, EC: $[-7 \div 7]$ (m/s^2). Meanwhile, the value range of the output variable damping force is defined as follows: f_{d1}, U: $[-1, 1 \div 1, 1]$ (N). Each input and output variable is quantified by 7 linguistic values: Negative Large: NL, Negative Middle: NM, Negative Small: NS, Zero: ZE, Positive Small: PS, Positive Middle: PM, and Positive Large: PL. The membership function form of fuzzy sets is selected in the form of trapezoid-trapmf and triangular-trimf. The membership function of the linguistic values for the input/output variables of the fuzzy inference system E, EC, U is shown in Figure 3.

The rule set of the fuzzy inference system E, EC, U is built to control the semiactive damping force to improve the ride comfort with 49 rules shown in Table 3. The communication relationship of the fuzzy inference system E, EC, U is the relationship between the input signals (E, EC) and the output signal (U) shown in Figure 4.

Table 2: Definition of linguistic variables for the controller.

Input variables	Output variables	Linguistic variables
$\dot{Z}_s$		E (e)
$\ddot{Z}_s$		EC (ec)
f_d	U (p)	

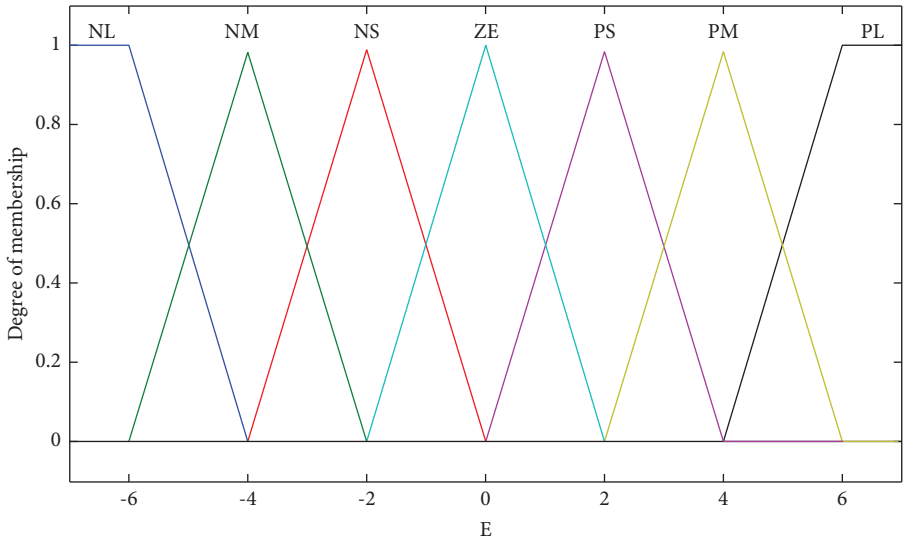

(a)

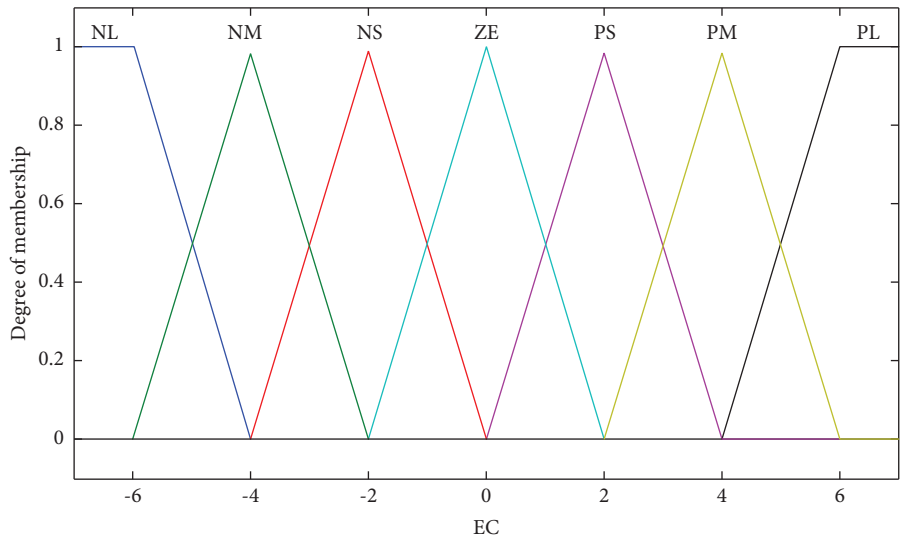

(b)

Figure 3: Continued.

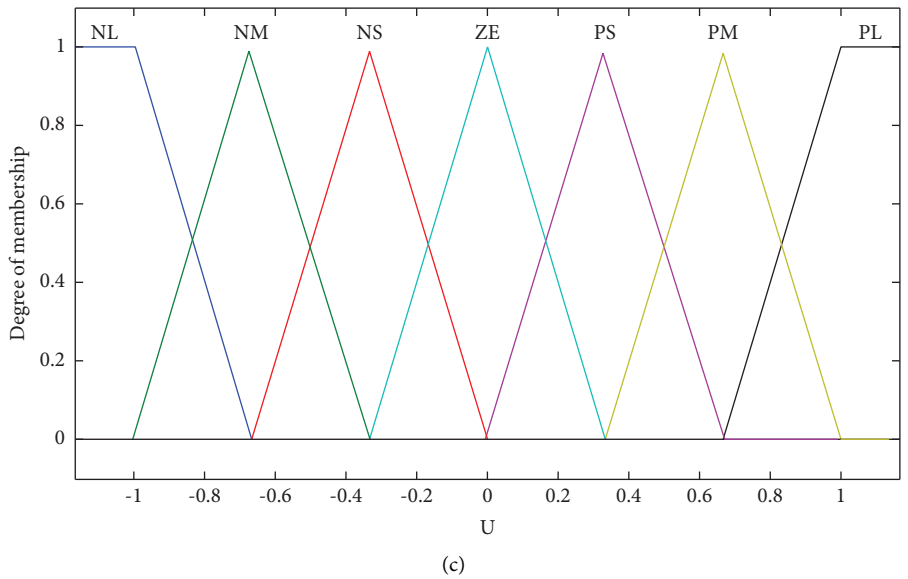

(c)

Figure 3: The membership function of the linguistic value for the input/output variables: (a) velocity of the sprung mass, E; (b) acceleration of the sprung mass, EC; (c) damping force, U.

Table 3: The rule set of the fuzzy inference system E, EC, U.

E	U EC						
	NL	NM	NS	ZE	PS	PM	PL
NL	PL	PL	PM	PS	PS	PS	ZE
NM	PL	PM	PS	PS	PS	ZE	NS
NS	PM	PS	ZE	ZE	ZE	NS	NM
ZE	PM	PS	ZE	ZE	ZE	NS	NM
PS	PM	PS	ZE	ZE	ZE	NS	NM
PM	PS	ZE	ZE	ZE	ZE	NM	NL
PL	ZE	NS	NS	NS	NM	NL	NL

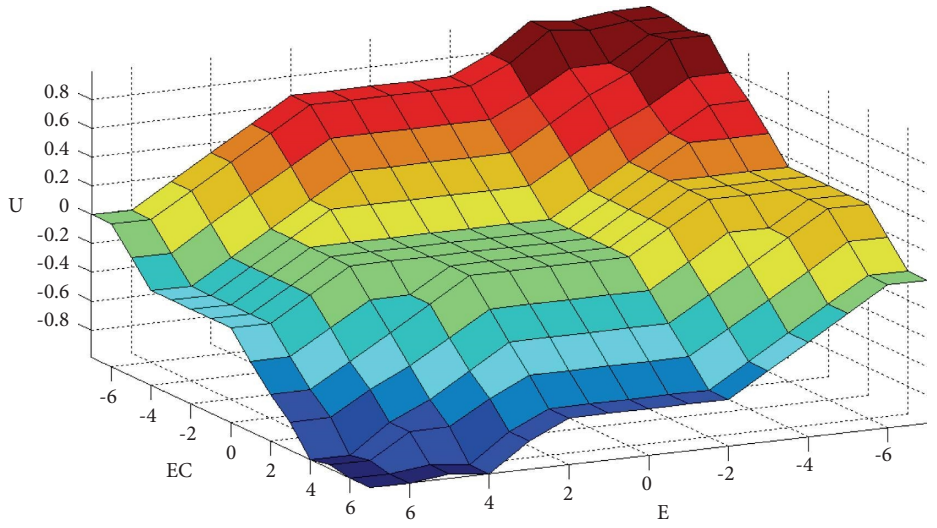

Figure 4: The communication relationship of the fuzzy inference system E, EC, U.

3.3. The Fuzzy Inference System e, ec, u. The physical value domain of the input/output variables is selected as follows: the velocity of the sprung mass $\dot{Z}_s$, e: $[-5 \div 5]$ (m/s), the acceleration of the sprung mass $\ddot{Z}_s$, ec: $[-6{,}3 \div 6{,}3]$ (m/s^2), and the damping force f_{d2}, u: $[-120 \div 120]$ (N). The input variables are quantified by 5 linguistic values: Negative Big:

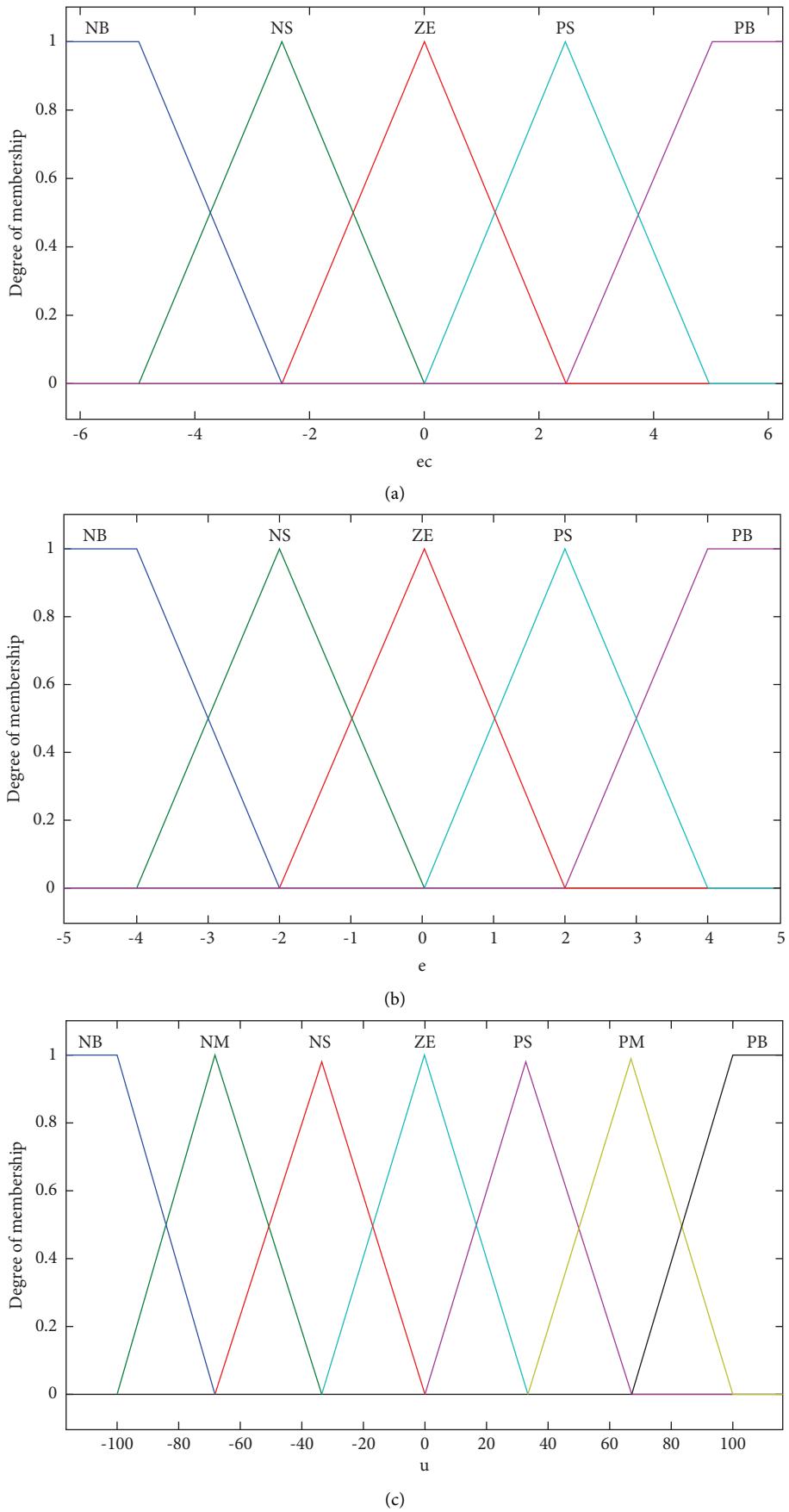

Figure 5: The membership function of the linguistic value for the input/output variables: (a) velocity of the sprung mass, *e*; (b) acceleration of the sprung mass, ec; (c) damping force, *u*.

Table 4: The rule set of the fuzzy inference system e, ec, u.

e	u ec				
	NB	NS	ZE	PS	PB
NB	ZE	ZE	ZE	ZE	ZE
NS	ZE	PS	ZE	NS	ZE
ZE	PM	PS	ZE	ZE	NM
PS	PM	PM	NS	NM	NM
PB	PS	PS	NS	NB	NB

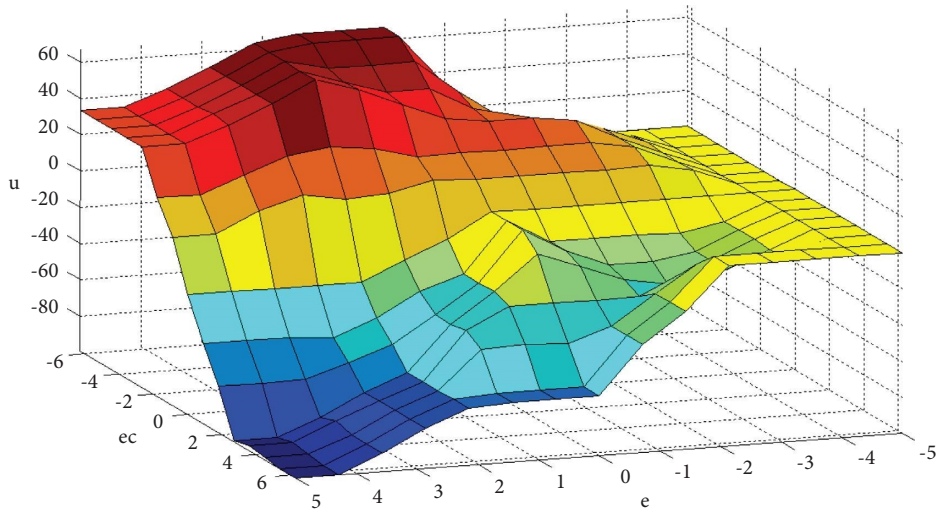

Figure 6: The communication relationship of the fuzzy inference system e, ec, u.

NB, Negative Small: NS, Zero-ZE, Positive Small: PS, and Positive Big: PB. Meanwhile, the output variable in the linguistic value is defined as in the fuzzy inference system E, EC, U. The membership function of the linguistic values for the input/output variables of the fuzzy inference system e, ec, u is shown in Figure 5. The rule set of the fuzzy inference system e, ec, u is built with 25 rules shown in Table 4. The communication relationship of the fuzzy inference system e, ec, u is shown in Figure 6.

3.4. Optimizing Fuzzy Controller. As mentioned in Subsection 3.1, the quality of the fuzzy controller for semiactive suspension system depends on the scaling factor for the defuzzification process (k_e and k_{ec}) and the scaling factor for the defuzzification process (k_u). The quality of control is assessed through the criterion of the root mean square (RMS) and from peak to peak of the acceleration of the sprung mass.

In this study, the author uses the least squares method (LQ). The goal of the nonlinear minimum variance is to find the optimal parameter set of the vector function $F(x)$ with the required parameter x according to equation (11), where $\|F(x)\|_2^2$ is defined as the square of the 2-norm [34].

$$\min_x \sum_{i=1}^{n} F_i(x)^2 = \min_x \|F(x)\|_2^2. \tag{11}$$

The optimal results using the LQ method for the fuzzy controller with a random road profile are determined as follows: $k_e = -10$, $k_{ec} = -1$, and $k_u = 21$.

4. Vibration Quality Analysis

4.1. Vibration Quality Analysis in the Frequency Domain. In order to evaluate the effectiveness of the fuzzy logic controller for the semiactive suspension system, the author investigates the excitation frequency up to 100 rad/s when comparing the fuzzy-controlled semiactive suspension system (solid line) with the four cases of the passive suspension system which have different damping coefficients (700, 1400, 3000, and 5000 Ns/m) [35, 36]. The simulation results in the frequency domain are characterized by the amplitude-frequency transfer function: the vertical displacement of the sprung mass (Figure 7), the vertical acceleration of the sprung mass (Figure 8), and the acceleration of the pitch angle (Figure 9).

Figure 7 shows the frequency-amplitude transfer function of the vertical displacement of the sprung mass. The resonance region is most pronounced in the frequency range from 5 to 8 rad/s. For a passive suspension system, as the damping coefficient increases, the vertical displacement of the sprung mass decreases. The effect of the semiactive suspension using the fuzzy controller is evident when the displacement of the sprung mass is reduced in most

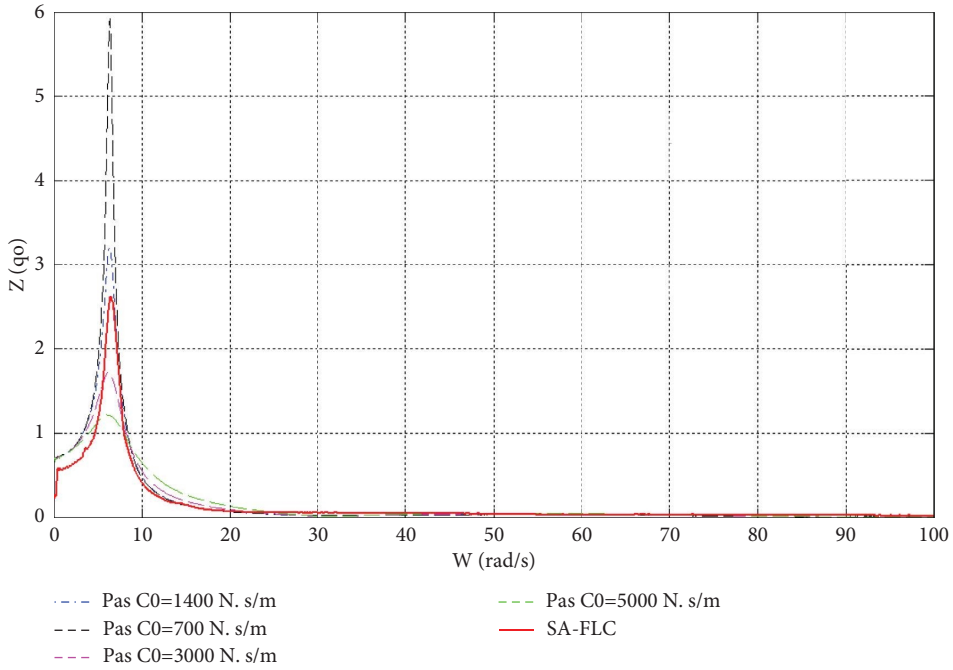

Figure 7: The amplitude-frequency transfer function of the vertical displacement of the sprung mass.

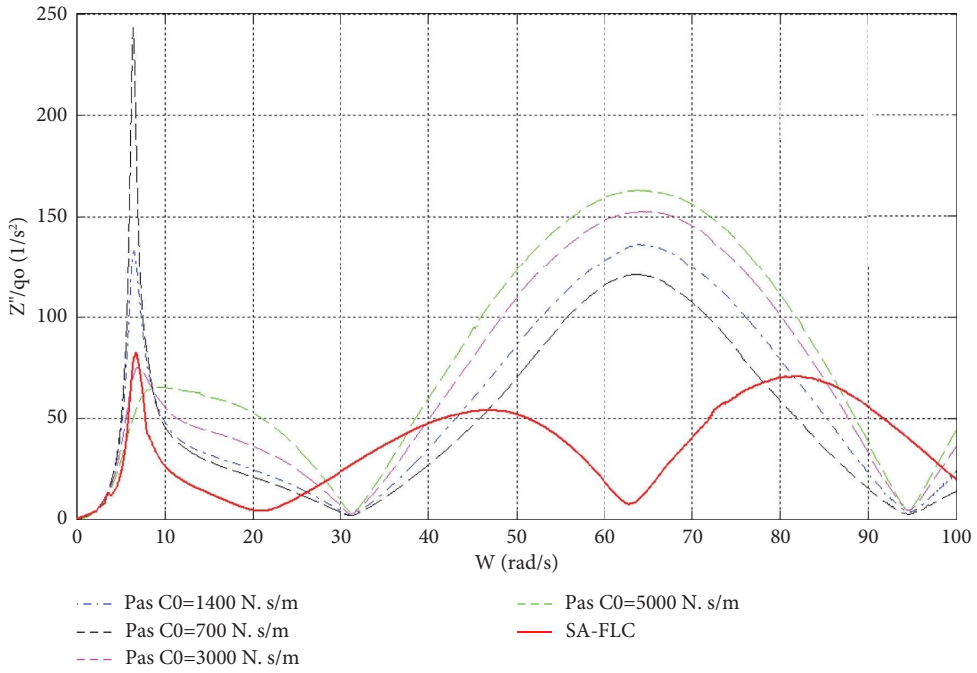

Figure 8: The amplitude-frequency transfer function of the vertical acceleration of the sprung mass.

frequency ranges from 0 to 100 rad/s. Figure 8 shows the frequency-amplitude transfer function of the vertical acceleration of the sprung mass. For the passive suspension, in the low-frequency resonant range (5–8 rad/s), when the damping coefficient increases, the acceleration decreases; however, in the high-frequency resonant range (50–80 rad/s), the system response is opposite. For the semiactive suspension with the fuzzy logic controller, the amplitude of the acceleration is reduced in both the low- and high-frequency resonance ranges. Figure 9 shows the frequency-amplitude transfer function of the acceleration of the pitch angle. The effect of the semiactive suspension with the fuzzy logic controller is well defined over most frequency ranges. Although in the frequency range from 58 rad/s to 70 rad/s, the amplitude is higher than that of the passive suspension system, and due to its very small value, it still

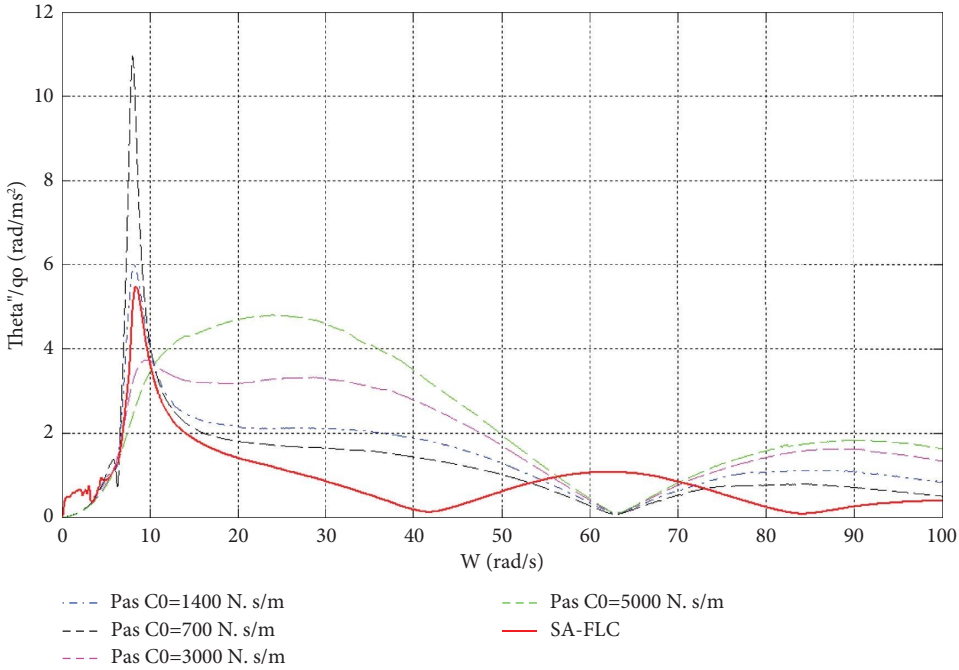

Figure 9: The amplitude-frequency transfer function of the acceleration of the pitch angle.

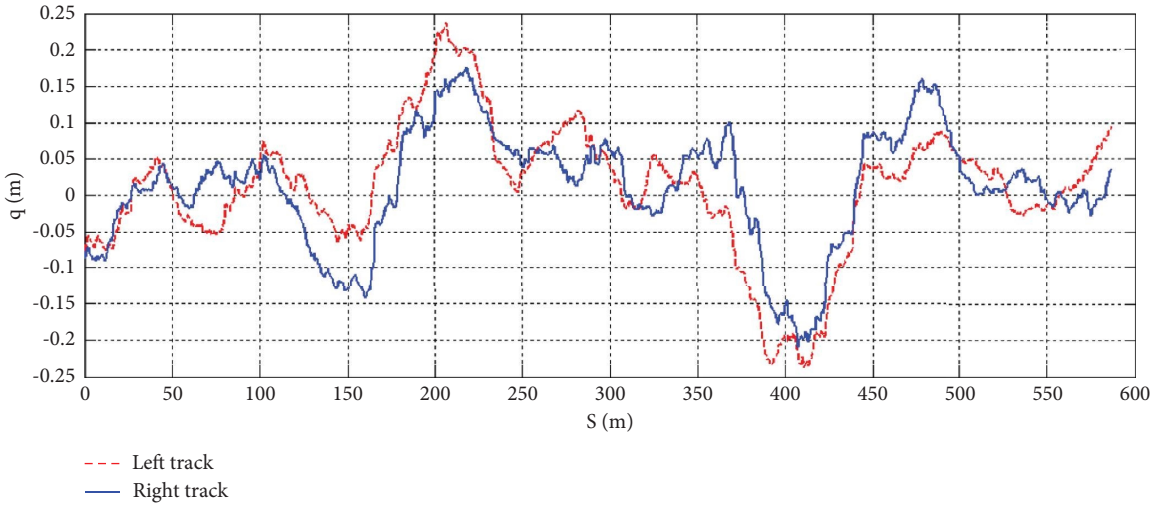

Figure 10: Random road profile measured in the Hanoi-Langson national road [32].

ensures the goal of improving the ride comfort. Thus, the simulation results on the frequency domain clearly show the effectiveness of the semiactive suspension with a fuzzy controller in improving the vibration quality of the cars.

4.2. Vibration Quality Analysis in the Time Domain. In the time domain, the author surveys with a random road profile of 600 m long on the Hanoi-Langson national highway [37] with a forward velocity of 50 km/h as shown in Figure 10. Survey results are evaluated through the magnitude value and the root mean square (RMS) value of displacement and acceleration of the sprung mass, acceleration of pitch and roll angles as shown in Figures from 11 to 14. It can be clearly seen that the magnitude values of the signals with time response in the case of using the semiactive suspension system with the fuzzy controller are reduced when compared with the passive suspension system. For the vertical displacement of the sprung mass, the RMS value reaches 0.0229, which is a decrease of 27%, while the value decreases about 36%, 43%, and 50%, respectively, of the three-direction acceleration of the sprung mass.

To evaluate in more detail the main criteria related to the ride comfort, this study evaluates the three displacements of the sprung mass and their acceleration ($Z_s, \theta, \phi, \ddot{Z}_s, \ddot{\theta}, \ddot{\phi}$), and the criteria related to the road holding is the interaction force

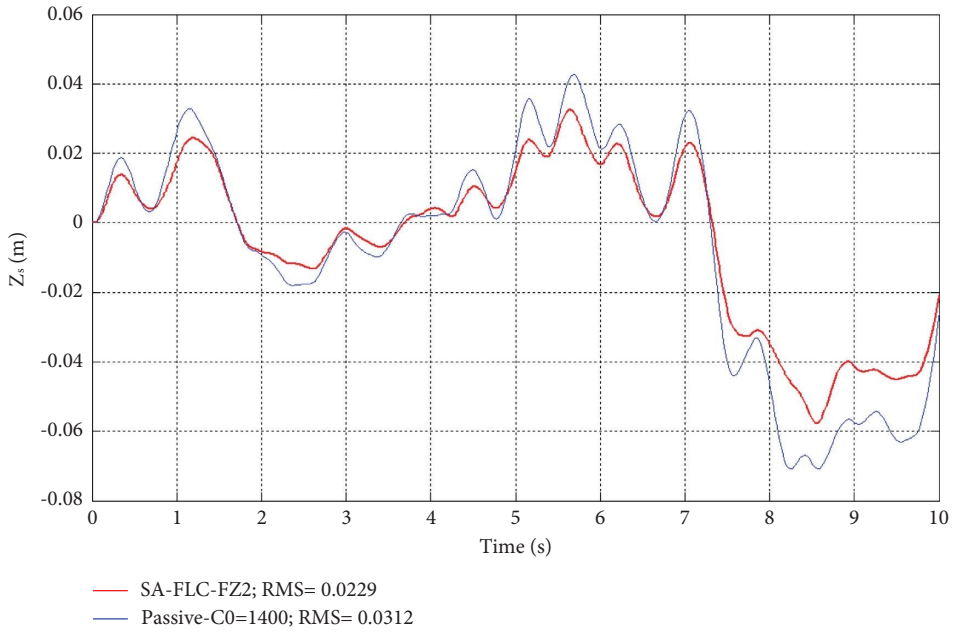

Figure 11: Time response of the vertical displacement of the sprung mass.

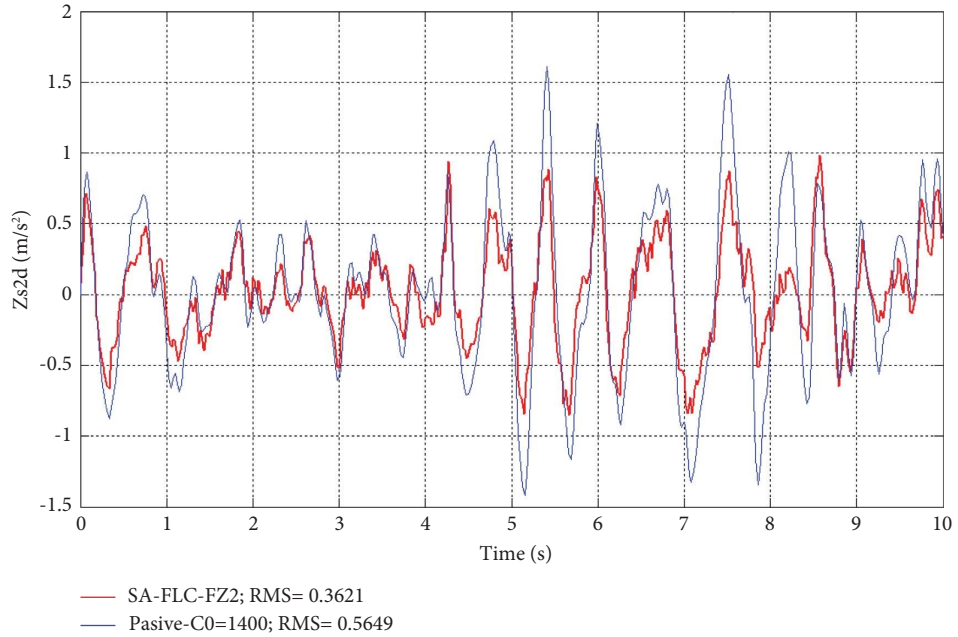

Figure 12: Time response of the vertical acceleration of the sprung mass.

of the four wheels acting on the road $(F_{dt1}, F_{dt2}, F_{dt3}, F_{dt4})$. The survey results in Figure 15 are compared through the RMS value, showing that the car using the semiactive suspension system with the fuzzy logic controller reduces the RMS value by over 25% compared to the passive suspension system. Specifically, the RMS values $\mathrm{RMS}(\ddot{Z}_s)$, $\mathrm{RMS}(\ddot{\phi})$, $\mathrm{RMS}(\ddot{\theta})$ are equal to 64.10%, 50.01%, and 56.61%, respectively, compared to the passive suspension system. Meanwhile, the RMS values $\mathrm{RMS}(F_{dt1})$, $\mathrm{RMS}(F_{dt2})$, $\mathrm{RMS}(F_{dt3})$, and $\mathrm{RMS}(F_{dt4})$ are equal to 73.91%, 70.78%, 69.18%, and 72.76% compared to the passive suspension system.

Figure 16 shows the time response of the forces generated by four semiactive dampers $(f_{d1}, f_{d2}, f_{d3}, \text{and} f_{d4})$. In this survey case, the damping forces move from −1050 N

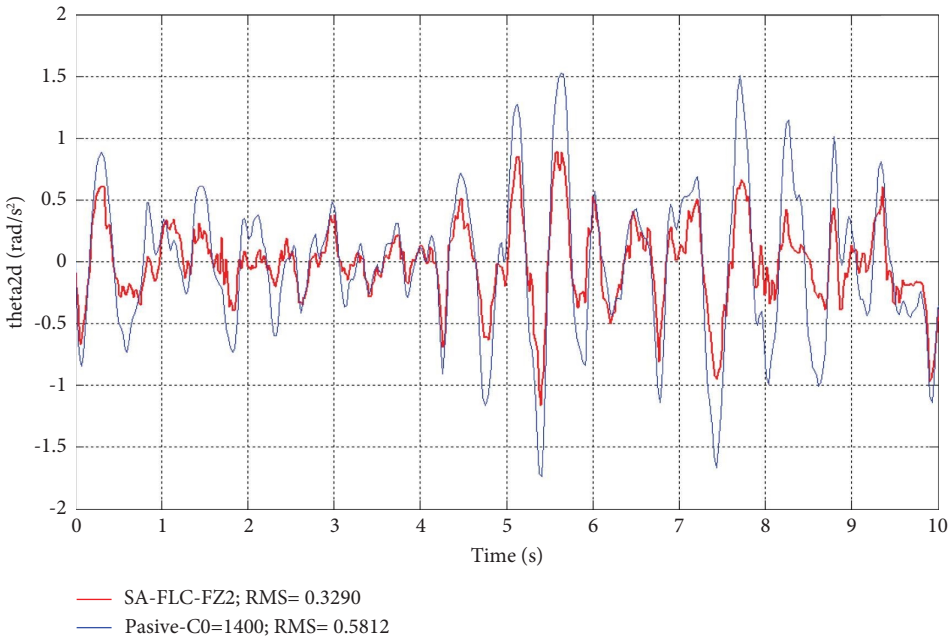

Figure 13: Time response of the acceleration of the pitch angle.

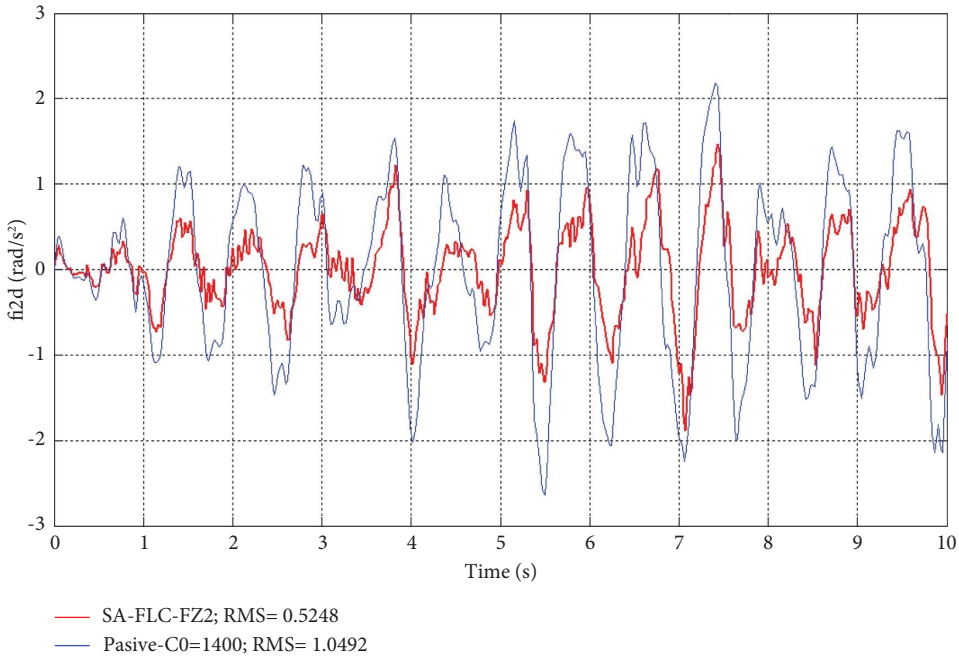

Figure 14: Time response of the acceleration of the roll angle.

to 700 N to ensure improved ride comfort of the car. The values of the forces change continuously according to the road profile states, which clearly show the advantages of the proposed control strategy.

Thus, the survey results in the frequency and time domains with the random road profile have shown that the car using a semiactive suspension with the fuzzy logic controller has improved the ride comfort, when compared to the car

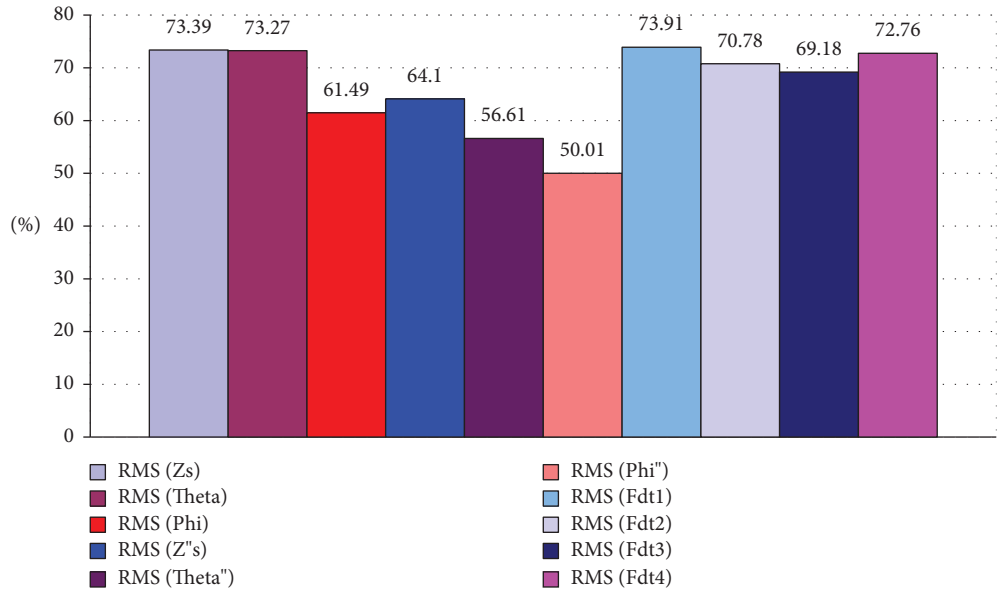

Figure 15: Graph to evaluate the quality of the car using a semiactive suspension system with the fuzzy logic controller compared to a passive suspension system.

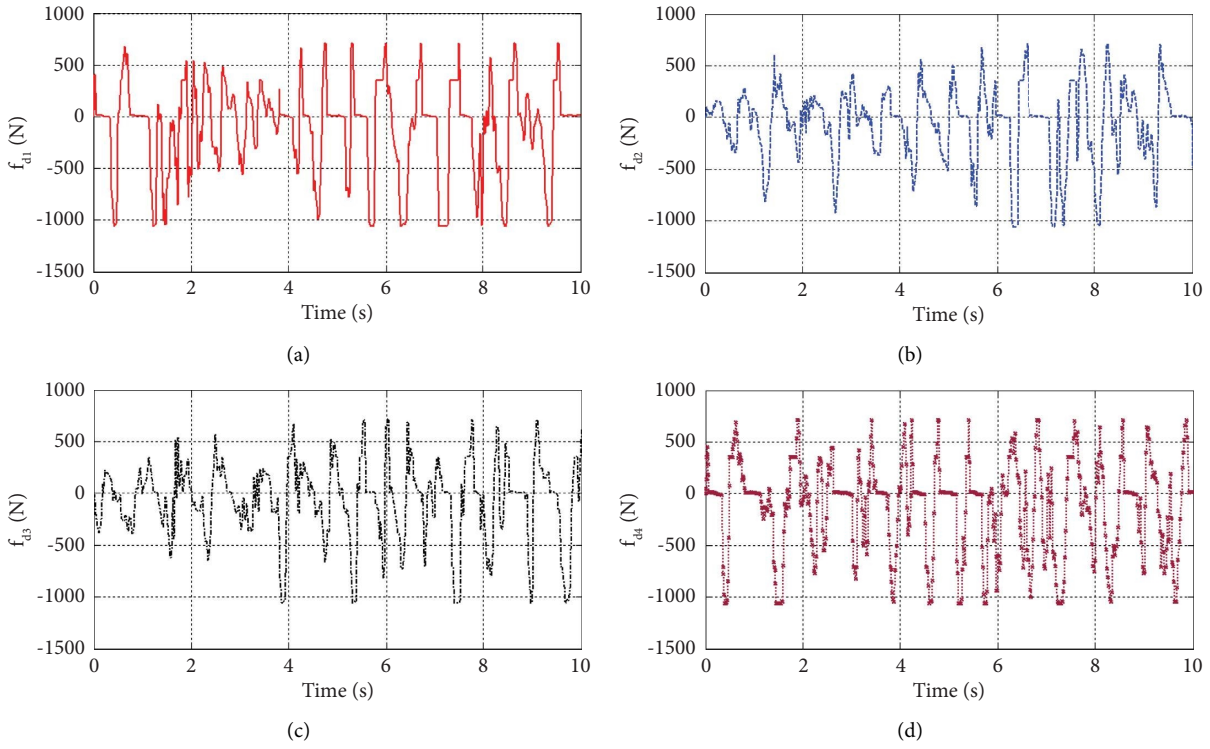

Figure 16: The time response of the forces of the semiactive dampers.

using the passive suspension system. In addition, the results of the evaluation of the displacement of the unsprung masses and the interaction forces of the four wheels acting on the road also indicate that the car using the semiactive suspension system has improved the road safety criteria. This confirms the outstanding advantage of the semiactive suspension with the proposed fuzzy logic controller.

5. Conclusions

Semiactive suspension systems are increasingly used in cars. In this paper, a full car model with 7 DOF is built, in which the semiactive suspension system is arranged at all four wheels. A two-layer parallel fuzzy logic controller is built with 49 rules for the first fuzzy inference system and 25 rules for the second fuzzy inference system. This fuzzy logic controller has the input of the signals related to the sprung mass, and the output is the damping force. As a result, the controller is capable of responding to a wide operating range of the system and allows for smoother force output. The simulation results are evaluated in the frequency and time domains. The results of the analysis with the random road profile have shown that the root mean square value of the signals when using the semiactive suspension with the fuzzy logic controller is reduced by more than 25% compared to the passive suspension system. Therefore, the proposed fuzzy logic controller has improved the ride comfort and the road safety and ensured the suspension space.

The next research direction that can be taken is to consider the nonlinearity of the MR or ER dampers in more detail in a closed-loop control structure. Comparing the effectiveness of this proposed control method with other control methods such as PID, LQR, and H_2/H_∞ is also a priority research direction in the coming time.

Data Availability

No data were used to support the findings of this study.

Conflicts of Interest

The author declares that there are no conflicts of interest.

References

[1] S. Fergani, *Robust multivariable control for vehicle dynamics*, Ph.D. thesis, Grenoble Alpes University, Grenoble, France, 2014.

[2] O. Sename, "Review on LPV approaches for suspension systems," *Electronics*, vol. 10, no. 17, pp. 2120–2123, 2021.

[3] S. Savaresi, C. Poussot-Vassal, C. Spelta, S. Olivier, and L. Dugard, *Semi-Active Suspension Control Design for Vehicles*, 1st edition, Elsevier, Amsterdam, Netherland, , 2010.

[4] A. Soliman and M. M. S. Kaldas, "Semi-active suspension systems from research to mass-market - a review," *Journal of Low Frequency Noise, Vibration and Active Control*, vol. 40, no. 2, pp. 1005–1023, 2019.

[5] G. TharehalliMata, H. Krishna, and M. Keshav, "Characterization of magneto-rheological fluid having elongated ferrous particles and its implementation in MR damper for three-wheeler passenger vehicle," *Part D: Journal of Automobile Engineering*, vol. 237, no. 2-3, pp. 426–439, 2022.

[6] G. Tharehalli mata, V. Mokenapalli, and H. Krishna, "Performance analysis of MR damper based semi-active suspension system using optimally tuned controllers," *Part D: Journal of Automobile Engineering*, vol. 235, no. 10-11, pp. 2871–2884, 2021.

[7] M. Menezes Morato, T.-P. Pham, O. Sename, and L. Dugard, "Development of a simple ER damper model for fault-tolerant control design," *Journal of the Brazilian Society of Mechanical Sciences and Engineering*, vol. 42, no. 10, p. 502, 2020.

[8] H. Hirani and C. S. Manjunatha, "Performance evaluation of a magnetorheological fluid variable valve," *Part D: Journal of Automobile Engineering*, vol. 221, no. 1, pp. 83–93, 2007.

[9] W. Elsaady, S. O. Oyadiji, and A. Nasser, "Evaluation of nonlinear dynamic phenomena in the hysteretic behaviour of magnetorheological dampers," *Applications in Engineering Science*, vol. 3, Article ID 100019, 2020.

[10] S. K. Priyatharrshan, T.-P. Pham, and O. Sename, "Identification and comparison of two nonlinear extended phenomenological models for an automotive ElectroRheological (ER) damper," *IFAC-PapersOnLine*, vol. 54, no. 7, pp. 439–444, 2021.

[11] D. Karnopp, M. J. Crosby, and R. A. Harwood, "Vibration control using semi-active force generators," *Journal of Engineering for Industry*, vol. 96, no. 2, pp. 619–626, 1974.

[12] C. Poussot-Vassal, O. Sename, L. Dugard, R. Ramirez-Mendoza, and L. Flores, "Optimal skyhook control for semi-active suspensions," *IFAC Proceedings Volumes*, vol. 39, no. 16, pp. 608–613, 2006.

[13] C. Liu, L. Chen, X. Yang, X. Zhang, and Y. Yang, "General theory of skyhook control and its application to semi-active suspension control strategy design," *IEEE Access*, vol. 7, pp. 101552–101560, 2019.

[14] C. F. Nicolas, J. Landaluze, E. Castrillo, M. Gaston, and R. Reyero, "Application of fuzzy logic control to the design of semi-active suspension systems," in *Proceedings of the 6th International Fuzzy Systems Conference*, vol. 2, pp. 987–993, Barcelona, Spain, July 1997.

[15] Y. Chen and M. P. Cartmell, "Hybrid fuzzy and sliding-mode control for motorised space tether spin-up when coupled with axial oscillation," *Journal of Physics: Conference Series*, vol. 181, Article ID 012093, 2009.

[16] X. Cao, L. Cao, and D. Wang, "The exact linearization and LQR control of semiactive connected hydropneumatic suspension system," *Journal of Control Science and Engineering*, vol. 2015, Article ID 690917, 10 pages, 2015.

[17] V. Van Tan, *Enhancing the roll stability of heavy vehicles by using an active anti-roll bar system*, Ph.D. thesis, Grenoble Alpes University, Grenoble, France, 2017.

[18] V. T. Vu, O. Sename, L. Dugard, and P. Gaspar, "Multi objective H_∞ active anti-roll bar control for heavy vehicles," *IFAC-PapersOnLine*, vol. 50, no. 1, pp. 13802–13807, 2017.

[19] M. Q. Nguyen, M. Canale, O. Sename, and L. Dugard, "A Model Predictive Control approach for semi-active suspension control problem of a full car," in *Proceedings of the IEEE 55th Conference on Decision and Control (CDC)*, pp. 721–726, Las Vegas, NV, USA, December 2016.

[20] H. E. Tseng and D. Hrovat, "State of the art survey: active and semi-active suspension control," *Vehicle System Dynamics*, vol. 53, no. 7, pp. 1034–1062, 2015.

[21] D. Hrovat, "Survey of Advanced Suspension Developments and Related Optimal Control Applications11This paper was not presented at any IFAC meeting. This paper was recommended for publication in revised form by Editor Karl Johan Åström.,22Simple, mostly LQ-based optimal control concepts gave useful insight about performance potentials, bandwidth requirements, and optimal structure of advanced vehicle suspensions. The present paper reviews these optimal control applications and related practical developments," *Automatica*, vol. 33, no. 10, pp. 1781–1817, 1997.

[22] V. T. Vu, O. Sename, L. Dugard, and P. Gáspár, "An investigation into the oil leakage effect inside the electronic

servo-valve for an H_∞/LPV active anti-roll bar system," *International Journal of Control, Automation and Systems*, vol. 17, no. 11, pp. 2917–2928, 2019.

[23] T.-P. Pham, O. Sename, L. Dugard, and V. T. Vu, "LPV force observer design and experimental validation from a dynamical semi-active ER damper model," *IFAC-PapersOnLine*, vol. 52, no. 17, pp. 60–65, 2019.

[24] V. T. Vu, O. Sename, L. Dugard, and P. Gaspar, "The design of an H_∞/LPV active braking control to improve vehicle roll stability," *IFAC-PapersOnLine*, vol. 52, no. 17, pp. 54–59, 2019.

[25] J. Yao and J. Zheng, "Semi-active suspension system design for quarter-car model using model reference sliding mode control," in *Proceedings of the 2006 IEEE International Conference on Vehicular Electronics and Safety*, pp. 398–402, Shanghai, China, December 2006.

[26] W. You, J. Lee, C. Lee, and K. Lee, "Semi-active control of a nonlinear quarter-car model of hyperloop capsule vehicle with Skyhook and Mixed Skyhook-Acceleration Driven Damper controller," *Advances in Mechanical Engineering*, vol. 13, no. 2, pp. 1–14, 2021.

[27] M. Ahmed and F. Svaricek, "Preview Control of Semi-active Suspension Based on a Half-Car Model Using Fast Fourier Transform," in *Proceedings of the 10th International Multi-Conferences on Systems, Signals & Devices*, pp. 1–6, Hammamet, Tunisia, June 2013.

[28] L. C. Félix-Herrán, D. Mehdi, J. Rodríguez-Ortiz, V. H. Benitez, R. A. Ramirez-Mendoza, and R. Soto, "Disturbance rejection in a one-half semi-active vehicle suspension by means of a fuzzy-H_∞ controller," *Shock and Vibration*, vol. 2019, Article ID 4532635, 14 pages, 2019.

[29] Z. Fang, W. Shu, D. Du, B. Xiang, Q. He, and K. He, "Semi-active suspension of a full-vehicle model based on double-loop control," *Procedia Engineering*, vol. 16, pp. 428–437, 2011.

[30] M. M. Morato, M. Q. Nguyen, O. Sename, and L. Dugard, "Design of a fast real-time LPV model predictive control system for semi-active suspension control of a full vehicle," *Journal of the Franklin Institute*, vol. 356, no. 3, pp. 1196–1224, 2019.

[31] M. Q. Nguyen, *LPV approaches for modelling and control of vehicle dynamics: application to a small car pilot plant with ER dampers*, Ph.D. thesis, Grenoble Alpes University, Grenoble, France, 2016.

[32] D. Wang, D. Zhao, M. Gong, and B. Yang, "Nonlinear predictive sliding mode control for active suspension system," *Shock and Vibration*, vol. 2018, Article ID 8194305, 10 pages, 2018.

[33] L. Li, L. Xu, H. Cui, M. A. A. Abdelkareem, Z. Liu, and J. Chen, "Validation and optimization of suspension design for testing platform vehicle," *Shock and Vibration*, vol. 2021, Article ID 7963517, 15 pages, 2021.

[34] J. Wolberg, *Data Analysis Using the Method of Least Squares*, Springer-Verlag Berlin Heidelberg, Berlin, Germany, 2006.

[35] C. S. Díaz-Choque, L. C. Félix-Herrán, and R. A. Ramírez-Mendoza, "Optimal skyhook and Groundhook control for semiactive suspension: a comprehensive methodology," *Shock and Vibration*, vol. 2021, Article ID 8084343, 21 pages, 2021.

[36] S. Kashem, R. Nagarajah, and M. Ektesabi, *Vehicle Suspension Systems and Electromagnetic Dampers*, Springer Singapore, Singapore, 2018.

[37] V. N. Tran, "Computer application to solve car vibration problems," University of Transport and Communications, Hanoi, Vietnam, University project T2003-CK-01, 2003.